PAPER

Multispectral computational ghost imaging with multiplexed illumination

To cite this article: Jian Huang and Dongfeng Shi 2017 *J. Opt.* **19** 075701

View the article online for updates and enhancements.

Related content

- The influence of the property of random coded patterns on fluctuation-correlation ghost imaging
  Chenglong Wang, Wenlin Gong, Xuehui Shao et al.

- Efficient single pixel imaging in Fourier space
  Liheng Bian, Jinli Suo, Xuemei Hu et al.

- Optical image encryption via high-quality computational ghost imaging using iterative phase retrieval
  Sui Liansheng, Cheng Yin, Li Bing et al.

Recent citations

- Low-cost single-pixel 3D imaging by using an LED array
  Eva Salvador-Balaguer *et al*

- High frame-rate computational ghost imaging system using an optical fiber phased array and a low-pixel APD array
  Chunbo Liu *et al*

- Simultaneous spatial, spectral, and 3D compressive imaging via efficient Fourier single-pixel measurements
  Zibang Zhang *et al*

Multispectral computational ghost imaging with multiplexed illumination

Jian Huang and Dongfeng Shi[1]

Key Laboratory of Atmospheric Composition and Optical Radiation, Anhui Institute of Optics and Fine Mechanics, Chinese Academy of Sciences, Hefei 230031, People's Republic of China

E-mail: jhuang@aiofm.ac.cn and dfshi@aiofm.ac.cn

Abstract

Computational ghost imaging has attracted wide attention from researchers in many fields over the last two decades. Multispectral imaging as one application of computational ghost imaging possesses spatial and spectral resolving abilities, and is very useful for surveying scenes and extracting detailed information. Existing multispectral imagers mostly utilize narrow band filters or dispersive optical devices to separate light of different wavelengths, and then use multiple bucket detectors or an array detector to record them separately. Here, we propose a novel multispectral ghost imaging method that uses one single bucket detector with multiplexed illumination to produce a colored image. The multiplexed illumination patterns are produced by three binary encoded matrices (corresponding to the red, green and blue colored information, respectively) and random patterns. The results of the simulation and experiment have verified that our method can be effective in recovering the colored object. Multispectral images are produced simultaneously by one single-pixel detector, which significantly reduces the amount of data acquisition.

Keywords: computational imaging, multispectral and hyperspectral imaging, image reconstruction techniques

(Some figures may appear in colour only in the online journal)

1. Introduction

Ghost imaging [1, 2] relies on the use of two correlated light fields and two detectors to create an image; one detector with no spatial resolution (such as a photomultiplier tube) is used to collect the light field which has previously interacted with an object, and the other detector with high spatial resolution is employed to collect the other correlated light which never interacts with the object. Neither of the detectors alone can produce an image of the object; however combining the measurements made by both detectors can shape an image. Computational ghost imaging [3] is developed from ghost imaging. In a computational ghost imaging system, the beam splitter and high spatial resolution detector are replaced by using a spatial light modulator capable of generating a programmable light field to illuminate the scene. The intensity structures are calculated and stored in computer memory rather than being measured by a detector with high spatial resolution. So only a single bucket photodetector is needed as an imaging device in a computational ghost imaging system. A single bucket detector has some significant advantages, such as high sensitivity, a wide spectrum range, low cost, small in size and light weight. So these advantages ensure that computational ghost imaging has great potential in many fields. Recently, it has made great progress and has already been put into practical applications, such as multilayer fluorescence imaging [4], optical encryption [5], remote sensing [6] and object tracking [7], etc.

Multispectral imaging which possesses spatial and spectral resolving abilities has attracted significant attention. Bian *et al* [8] proposed that by utilizing the fast response of the detector, the 3D spatial–spectral information from the scene can be multiplexed into a dense 1D measurement sequence and then demultiplexed computationally under the single-pixel imaging scheme. Wang *et al* [9] proposed a temporal multiplexing scheme for hyperspectral computational ghost imaging. They proposed a spectrum-encoded

---

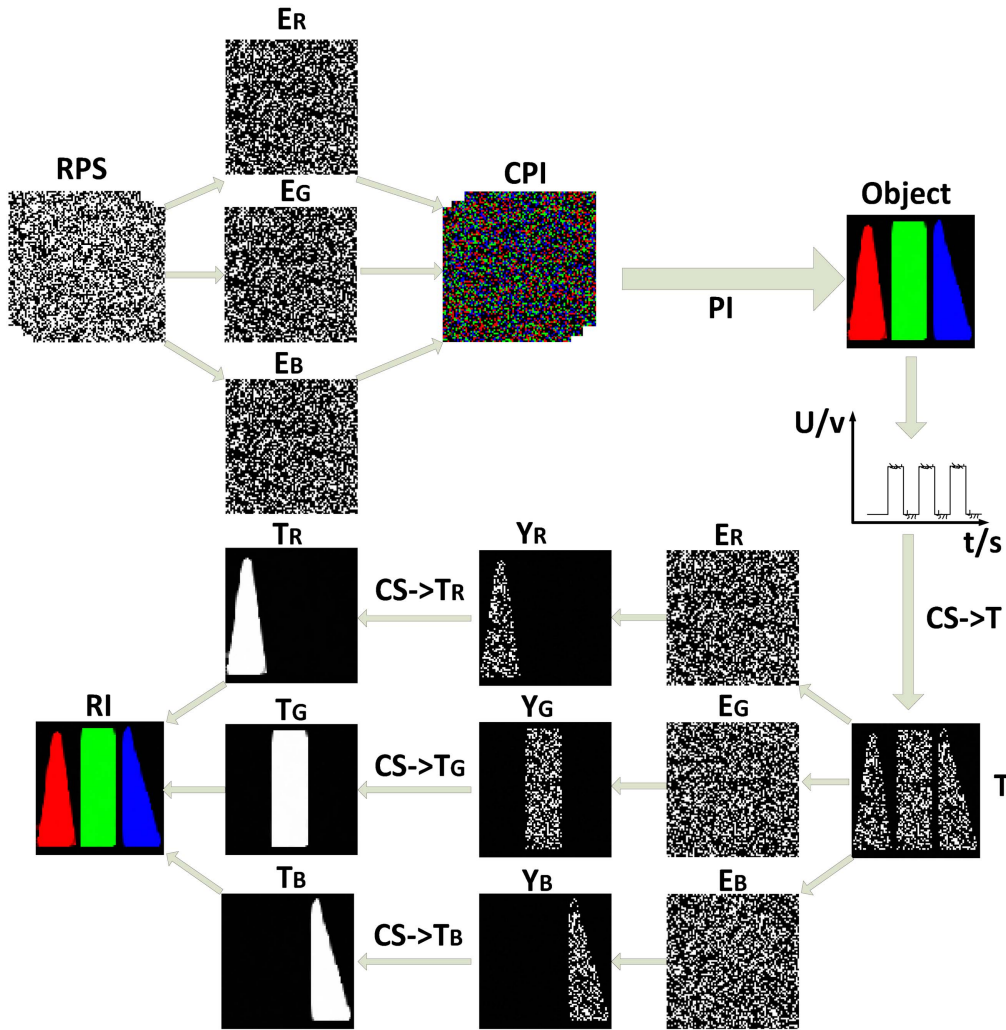[1] Authors to whom any correspondence should be addressed.

Figure 1. Procedure of our method for reconstructing an object. RPS: random patterns, *S*; CPI: colored patterns, *I*; PI: projection illumination; CS- > *T*: solve *T* based on equation (5); CS- > T_R, CS- > T_G and CS- > T_B: compute T_R, T_G, and T_B, based on equation (8); RI: recovered image.

acquisition scheme to achieve the computational ghost imaging of hyperspectral data. Taking advantage of the speed gap between the extremely fast response of the bucket detector and the lower magnitude spatial illumination modulation, their approach temporally multiplexes a group of diverse spectra into each elapsed 2D illumination pattern. Welsh *et al* [10, 11] employed a digital light projector in a computational ghost imaging system with multiple spectrally-filtered photodetectors to simultaneously obtain the red, green and blue colored planes. The imaging system can obtain multi-wavelength reconstructions of real objects.

Most of the natural scenes have sparse characteristics under some transformations based on compression theory, and they can be recovered exactly from a relatively small number of measurements. Furthermore, full sampling information regarding the imaging object can be reconstructed under random sampling by employing a compressed sensing algorithm [12]. In this paper, we demonstrate a novel multispectral ghost imaging method that uses one single bucket detector with multiplexed illumination to produce a colored

image. The multiplexed illumination patterns are produced by three binary encoded matrices (corresponding to red, green and blue colored information, respectively) and random patterns. We investigated the proposed method numerically and experimentally. The results of the simulation and experiment confirm that our method is effective.

2. Method of multispectral image reconstruction

In general, iterative and compressed sensing algorithms are the two main types of reconstruction algorithms that can be employed in processing the acquired data in a computational ghost imaging system. An iterative algorithm utilizes an entire data set in a bulk process to find the best solution for a set of unknowns [10], while compressed sensing algorithms utilize less than 30% of Nyquist limit measurements to extract the objects [13]. So, here, we apply a compressed sensing algorithm for our imaging reconstruction.
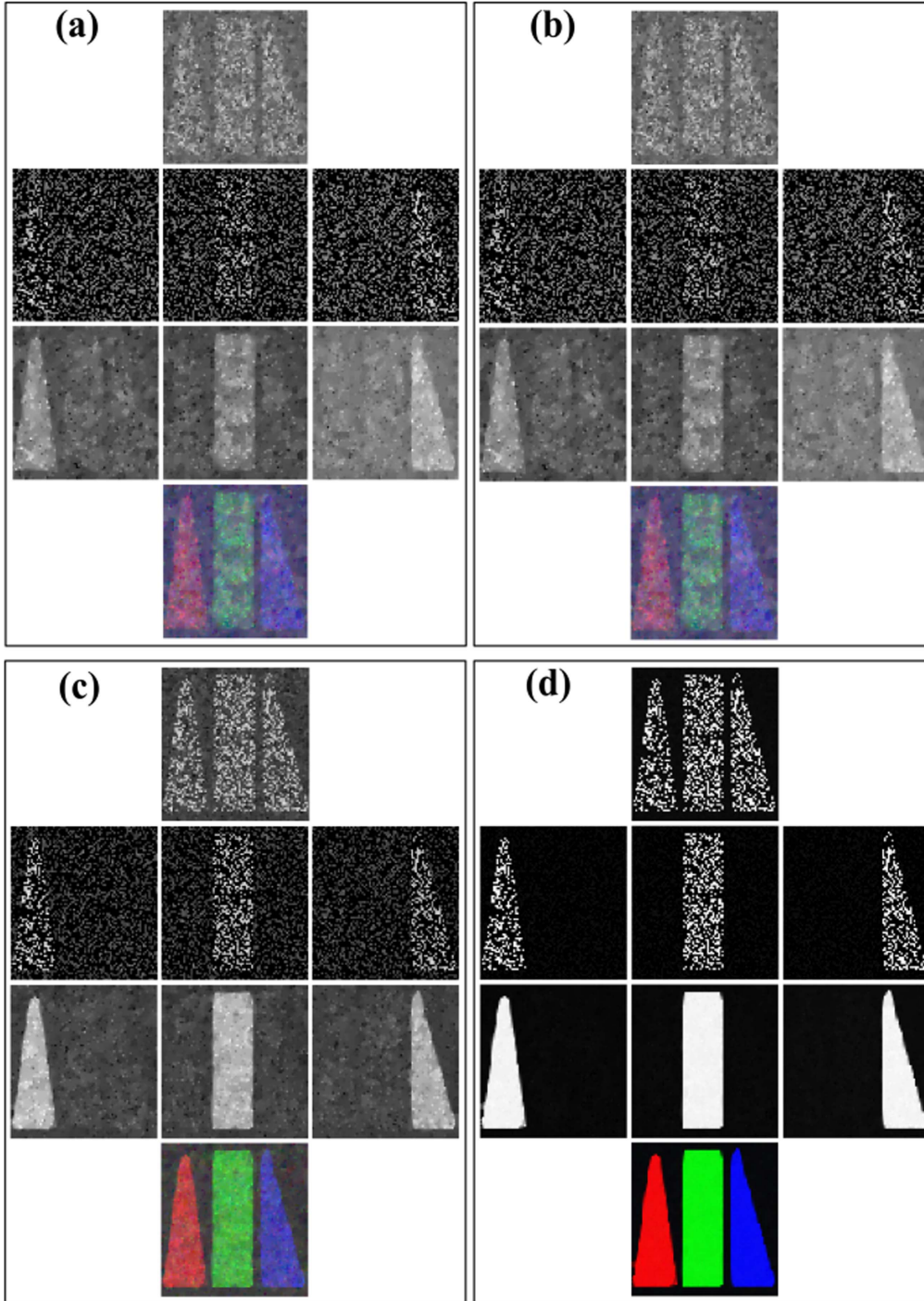
Figure 2. Simulation results of the imaging of a colored object under different measurements. (a) The result of 3000 measurements. (b) The result of 3500 measurements. (c) The result of 4000 measurements. (d) The result of 4500 measurements.

In our proposed method, the multiplexed illumination patterns are color mixed. Firstly, three $N \times N$ encoded matrices named E_R, E_G and E_B are produced by a computer program, and the three encoded matrices should abide by some properties, as follows:

(1) E_R, E_G and E_B are binary matrices.
(2) $E_R + E_G + E_B = E$.
(3) $E_m \cdot E_n = \begin{cases} 0 & m \neq n \\ E_m & m = n \end{cases}$ $m, n = R, G, B$.

That means the three encoded matrices are orthogonal and all the elements of E are equal to 1. For ith projection, a random $N \times N$ pattern $S_i(x, y)$ is used to produce a multiplexed illumination pattern I_i which fuses the three products of the random pattern and the encoded matrices, as follows:

$$I_i = E_R \cdot S_i(x, y) + E_G \cdot S_i(x, y) + E_B \cdot S_i(x, y). \quad (1)$$

$E_R \cdot S_i(x, y)$, $E_G \cdot S_i(x, y)$ and $E_B \cdot S_i(x, y)$ will be simultaneously loaded into the projection system. Then the multiplexed
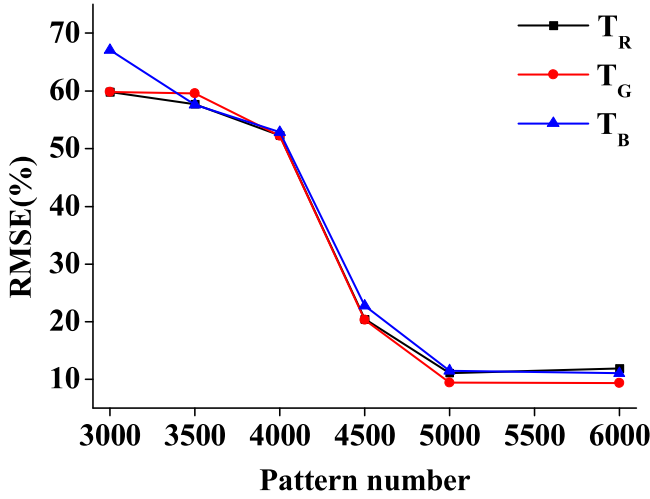
Figure 3. The plot of RMSE with respect to pattern numbers.

illumination pattern will be projected onto the object under a certain frequency and the corresponding reflected intensity is detected by a single-pixel photodetector. The measured signal U_i can be expressed as follows:

$$U_i = \sum_{N \times N} (C_R \cdot E_R \cdot S_i \cdot T_R + C_G \cdot E_G \cdot S_i \cdot T_G$$
$$+ C_B \cdot E_B \cdot S_i \cdot T_B). \tag{2}$$

Here, T_R, T_G and T_B are the red, green and blue information of the imaging scene, respectively. C_R, C_G and C_B represent correction coefficients of the single-pixel detector responding to the red, green and blue light, respectively, which can be gained by spectrum calibration, and the symbol $\sum_{N \times N}$ represents that the $N \times N$ elements of the matrix are summed. equation (2) can be rearranged as below:

$$U_i = \sum_{N \times N} S_i \cdot T. \tag{3}$$

Here, T is the fused information of the imaging scene, and can be expressed as $T = C_R \cdot E_R \cdot T_R + C_G \cdot E_G \cdot T_G + C_B \cdot E_B \cdot T_B$. For M projections, equation (3) can be simplified as below:

$$S \cdot T = U. \tag{4}$$

Here, U is a measurement signal vector of $M \times 1$; the random patterns S are reshaped to $M \times N^2$, and the object information T is a vector of $N^2 \times 1$. Under the condition $M \ll N$, it seems hopeless to solve the object information T since the number of equations is much smaller than the number of unknown variables. However, most of the time T is compressible, and can be accurately recovered under the condition $M \ll N$. Here, we use a second-order cone program of min-TV with quadratic constraints (available at www.l1-magic.org) to solve T. The constrained linear equation turns into the following optimization:

$$\min \ TV(T) \ \text{subject to} \ \ \|S \cdot T - U\|_2 \leqslant \gamma. \tag{5}$$

The specified parameter γ is set to 0.01. Once T is recovered, T_R, T_G and T_B can be extracted by making use of the property of E_R, E_G and E_B as below:

$$E_R \cdot T = E_R \cdot (C_R \cdot E_R \cdot T_R + C_G \cdot E_G \cdot T_G + C_B \cdot E_B \cdot T_B)$$
$$E_G \cdot T = E_G \cdot (C_R \cdot E_R \cdot T_R + C_G \cdot E_G \cdot T_G + C_B \cdot E_B \cdot T_B)$$
$$E_B \cdot T = E_B \cdot (C_R \cdot E_R \cdot T_R + C_G \cdot E_G \cdot T_G + C_B \cdot E_B \cdot T_B). \tag{6}$$

Then, equation (6) can be sorted out and simplified as follows:

$$Y_R = E_R \cdot T = (C_R \cdot E_R) \cdot T_R$$
$$Y_G = E_G \cdot T = (C_G \cdot E_G) \cdot T_G$$
$$Y_B = E_B \cdot T = (C_B \cdot E_B) \cdot T_B. \tag{7}$$

Here, Y_R, Y_G and Y_B are known $N \times N$ matrices which can be reshaped to $N^2 \times 1$ matrices, respectively, and $C_R \cdot E_R$, $C_G \cdot E_G$ and $C_B \cdot E_B$ are also known $N \times N$ matrices which can be reshaped to an $N^2 \times N^2$ diagonal matrix. T_R, T_G and T_B are $N^2 \times 1$ matrices. In order to exactly capture the full sampling information of the imaging object, optimizations can be resorted to, as follows:

$$\min \ TV(T_m) \ \text{subject to} \ \ \|(C_m \cdot E_m) \cdot T_m - Y_m\|_2 \leqslant \delta$$
$$m = R, G, B. \tag{8}$$

Here, the specified parameter δ is set to 0.01. Finally, T_R, T_G and T_B are reshaped to $N \times N$ matrices, and the final reconstructed colored image can be produced by fusing T_R, T_G and T_B.

The whole procedure of the proposed method is demonstrated in figure 1. First, the computer program produces three binary encoded matrices E_R, E_G, E_B and random patterns S. The multiplexed illumination colored patterns I are produced by fusing the product of random patterns and the three encoded matrices. They are loaded into the projection system, and then projected onto the scene. The reflected light intensity U is collected by a single-pixel photodetector. The fused information from the scene T can be restored by equation (5). Then, T is separated into three parts which are named Y_R, Y_G and Y_B, indicating the red, green and blue information under partial random sampling, respectively. The full sampling information of the red, green and blue reflected from the scene named T_R, T_G and T_B can be recovered by equation (8). Finally, the colored image will be reconstructed by integrating the full sampling information of the red, green and blue reflected information.

3. Experimental verification

3.1. Quantitative research on simulation

In order to evaluate our method, we designed a colored object (with a pixel resolution of 81×81) containing three parts: a red isosceles triangle, a green rectangle and a blue right triangle. The simulation results are shown in figure 2 which demonstrates the recovered results under 3000, 3500, 4000 and 4500 measurements, respectively. In figures 2(a)–(d), the first row shows the fused information of the imaging object T. The results of the red,
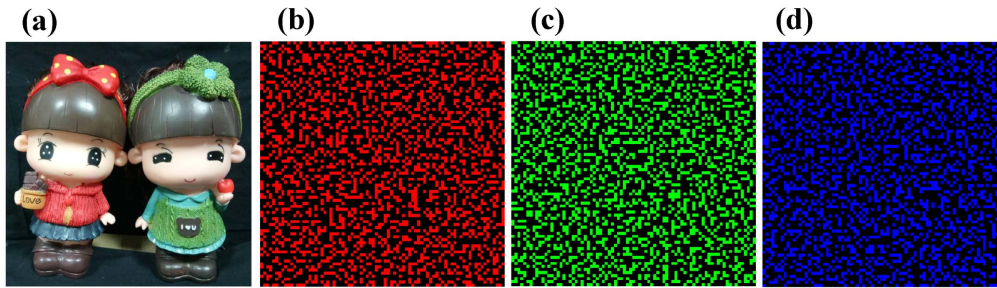
Figure 4. (a) The imaging target. (b) The encoded matrix of red showing in the red level. (c) The encoded matrix of green showing in the green level. (d) The encoded matrix of blue showing in the blue level.
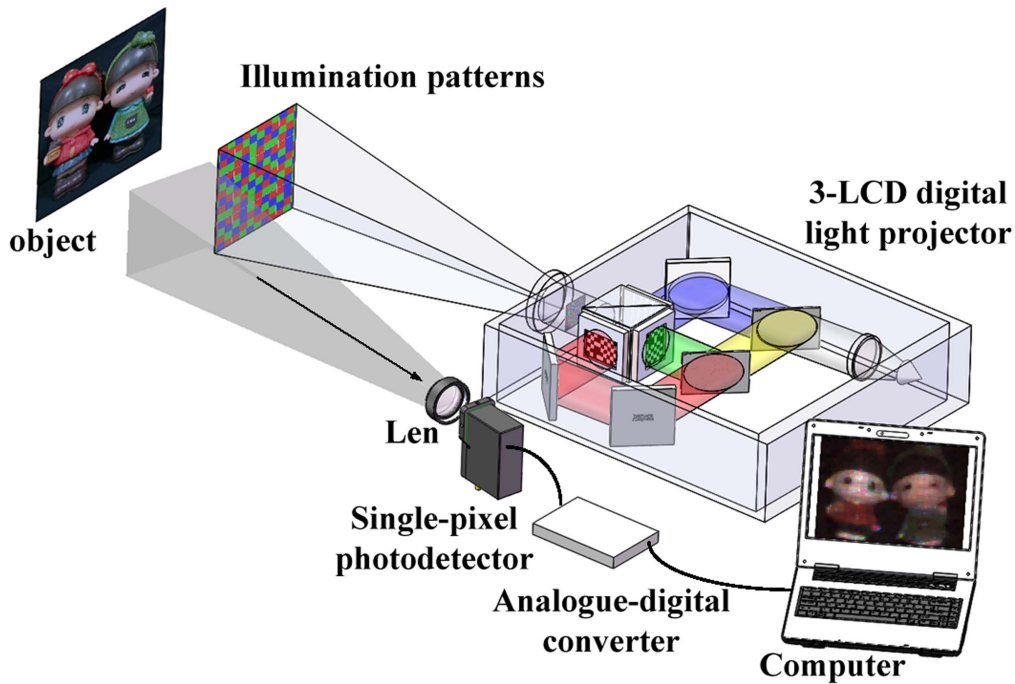

Figure 5. Schematic of our experimental system.

green and blue information under partial random sampling in the gray level are shown in the second row (from left to right), which are separated by the three encoded matrices E_R, E_G, E_B and the information T, respectively. The third row (from left to right) shows the full sampling results of the red, green and blue information of the colored object in the gray level. The fourth row shows the final reconstruction result of the imaging object. In this paper, the number of 1's in the three binary matrices E_R, E_G and E_B is equal to 2187 which is one-third of the total pixels of the imaging object. Of course, the number of 1's in the three binary matrices need not be equal in some other situation. From the simulation results, we can see that the recovered quality gets better when the illumination patterns increase. Figure 3 is the plot of the RMSE (root mean square error) with respect to the pattern numbers for the quantitative analysis in our method. The RMSE of T_R, T_G and T_B are almost constant when the measurements exceed 5000. The results of the simulation show that our method can distinguish the specific colored information and reconstruct the colored object via multiplexed illumination.

3.2. Experimental study

Next, an experimental system was built in the laboratory environment to test our method .The imaging object is depicted in figure 4(a). The red, green and blue encoded matrices are shown in figures 4(b)–(d), respectively. The multiplexed illumination patterns, which were employed in the simulation experiment, are projected onto the imaging object. The multispectral computational ghost imaging setup is shown in figure 5. The commercial digital light projector (SONY 3-LCD VPL-CX131) illuminates the object with the multiplexed patterns. The 3-LCD projector contains an ultrahigh voltage mercury lamp which produces white light; two dichroic mirrors can separate the white light into red, green and blue light which will transmit onto the corresponding LCDs. The LCDs can be programmed by a computer programmer, respectively. The detection unit (a photomultiplier, THORLABS PMM02-1, 280–850 nm) collects the reflected light from the object. An analogue to digital converter (NI USB-6211, maximum sampling rate is 250 k s^{-1} for
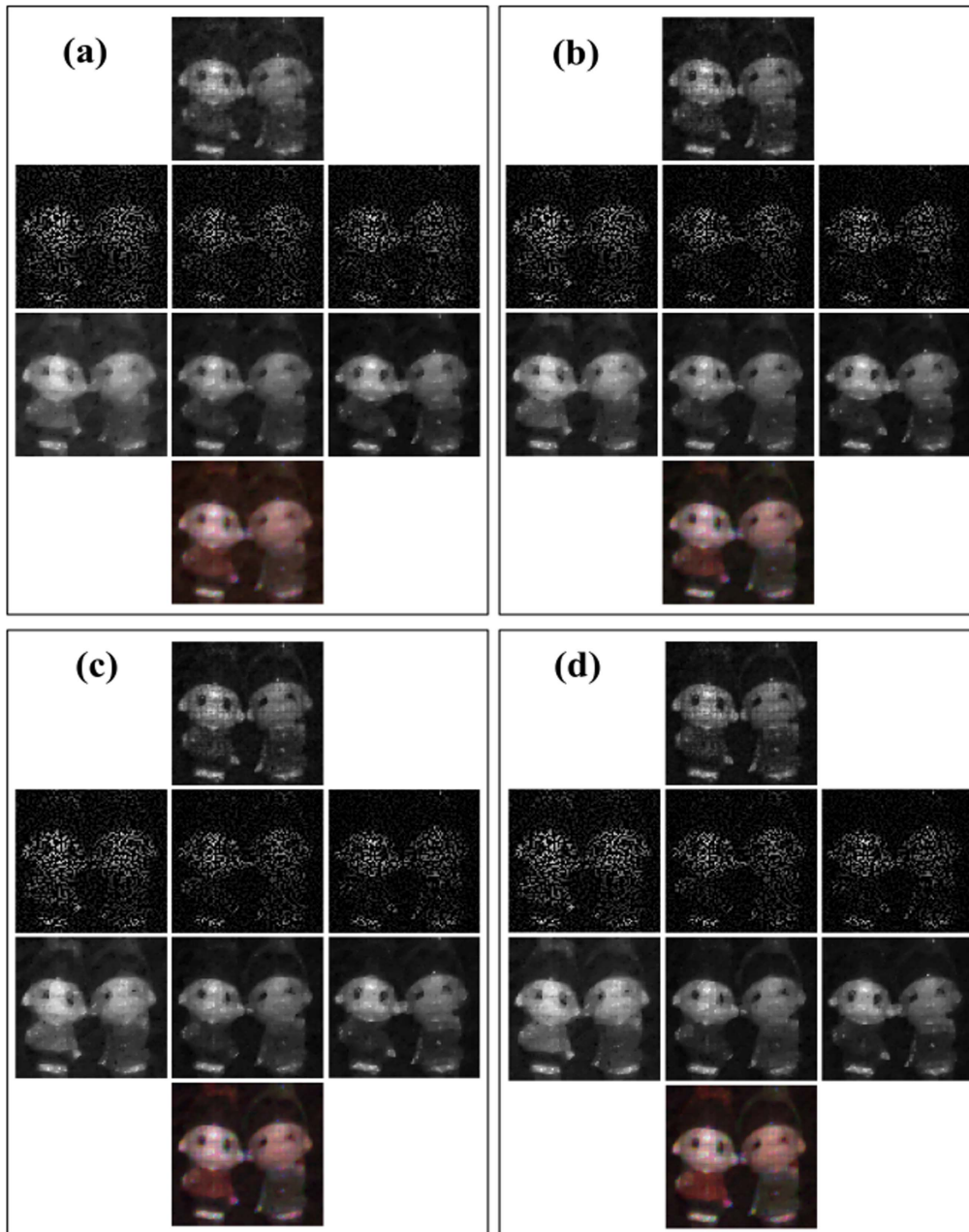
Figure 6. Experimental results of the imaging of two adjacent colored figures under different measurements. (a) The result of 3000 measurements. (b) The result of 4000 measurements. (c) The result of 5000 measurements. (d) The result of 6000 measurements.

a single channel) is used to digitize the detected signal and a computer is employed to generate the illumination patterns and perform multispectral reconstructions of the test object. The corresponding experimental results are shown in figure 6. The pixel resolution of the imaging is 81×81. The rank sequences of the experimental results are the as same as the simulation results in figure 2. From the experimental results shown in figure 6, we find that the quality of the recovered results are enhanced as the measurements increase. The experimental results confirm that our method is effective. However, there are some differences between the recovered results of the simulation and experiment. The possible reasons are as follows: (1) The imaging object is binary in the simulation, while the experimental imaging object is gray;

(2) there are possibly some disturbances (such as electronic noise, stray light, etc) in the experimental environment, while the noises are neglected in the simulation.

The results of the simulation and experiment have shown that our method can recover the colored object, and the quality of the recovered multispectral image gets better as the measurements increase. Of course, the quality of the recovered image in the experiment can be further improved by other approaches, such as the application of 2D orthogonal sinusoidal patterns instead of random patterns in [14] when the image of the object contains mainly low spatial frequencies. Our method has some superiority: one is that multispectral images are produced simultaneously by one single-pixel detector which makes our system more compact

and robust; the other one is that the red, green and blue information are encoded by the three binary matrices, which is crucial for recovering the multispectral image. The imaging object cannot be exactly recovered if the encoded matrices are inaccurate. Therefore, our proposed method can also be applied in information encryption.

In this paper, a proposed method is introduced to perform the imaging of three wavelength bands (which are set to standard visible red, green and blue). A commercial digital light projector is employed to achieve multispectral imaging in our imaging system. We cannot adjust its configuration to change the wavelength bands or increase the number of wavelength bands in the existing set-up. The wavelength bands can be changed by adjusting the corresponding color separation filters in the redesigned optical illumination system. Our method can also be extended to more than three wavelengths by redesigning the optical system. The main change is to adjust the corresponding optical illumination system and the binary encoded matrices. An example is provided below to achieve eight wavelength bands. Suppose the imaging pixel resolution is 80×80. First, it is necessary to produce eight binary encoded matrices. The eight encoded matrices are orthogonal, and the number of 1's in each encoded matrix is 800. That is to say, the sampling rate of the single wavelength bands is 12.5%. The multiplexed illumination patterns are produced by eight encoded matrices (corresponding to eight wavelength bands, respectively) and random patterns. Then, it needs eight independent light modulators and eight optical filters and beam combinations in the new optical system in order to project the 8-wavelength-band multiplexed illumination patterns. The image recovery technique is similar to the three wavelength bands described in detail in section 2.

4. Conclusions

In summary, we have proposed and validated a novel multi-spectral computational ghost imaging method with multi-plexed illumination. The multiplexed illumination patterns are produced by three binary encoded matrices (corresponding to red, green and blue colored information, respectively) and random patterns. In order to exactly recover the multispectral imaging object, compressed sensing algorithms are employed four times in our reconstructed procedure, so it is still slightly time consuming. The next focus is to improve the efficiency of the recovered algorithms. Besides, in the simulation and experiment, we have found that the imaging quality is easily

influenced by the three binary encoded matrices which are crucial to accomplish multiplexed illumination, so future research will aim to optimize the encoded matrices.

Acknowledgments

References

[1] Pittman T B, Shih Y H, Strekalov D V and Sergienko A V 1995 Optical imaging by means of 2-photon quantum entanglement *Phys. Rev.* A **52** R3429–32

[2] Ferri F, Magatti D, Gatti A, Bache M, Brambilla E and Lugiato L A 2005 High-resolution ghost image and ghost diffraction experiments with thermal light *Phys. Rev. Lett.* **94** 183602

[3] Shapiro J H 2008 Computational ghost imaging *Phys. Rev.* A **78** 061802

[4] Guo K K, Jiang S W and Zheng G A 2016 Multilayer fluorescence imaging on a single-pixel detector *Biomed. Opt. Express* **7** 2425–31

[5] Clemente P, Duran V, Torres-Company V, Tajahuerce E and Lancis J 2010 Optical encryption based on computational ghost imaging *Opt. Lett.* **35** 2391–3

[6] Zhao C Q, Gong W L, Chen M L, Li E R, Wang H, Xu W D and Han S S 2012 Ghost imaging lidar via sparsity constraints *Appl. Phys. Lett.* **101** 141123

[7] Li E R, Bo Z W, Chen M L, Gong W L and Han S S 2014 Ghost imaging of a moving target with an unknown constant speed *Appl. Phys. Lett.* **104** 3600

[8] Bian L H, Suo J L, Situ G H, Li Z W, Fan J T, Chen F and Dai Q H 2016 Multispectral imaging using a single bucket detector *Sci. Rep-UK* **6** 24752

[9] Wang Y W, Suo J L, Fan J T and Dai Q H 2016 Hyperspectral computational ghost imaging via temporal multiplexing *IEEE Photonic Tech.* L **28** 288–91

[10] Welsh S S, Edgar M P, Bowman R, Jonathan P, Sun B Q and Padgett M J 2013 Fast full-color computational imaging with single-pixel detectors *Opt. Express* **21** 23068–74

[11] Welsh S S, Edgar M P, Jonathan P, Sun B Q and Padgett M J 2013 *Proc. SPIE* **8618** 86180I

[12] Gao L, Liang J Y, Li C Y and Wang L H V 2014 Single-shot compressed ultrafast photography at one hundred billion frames per second *Nature* **516** 74–U159

[13] Zerom P, Chan K W C, Howell J C and Boyd R W 2011 Entangled-photon compressive ghost imaging *Phys. Rev.* A **84** 061804

[14] Khamoushi S M M, Nosrati Y and Tavassoli S H 2015 Sinusoidal ghost imaging *Opt. Lett.* **40** 3452–5